Journal of ELECTRONIC MATERIALS
https://doi.org/10.1007/s11664-019-07496-w

First-Principle Computed Structural and Thermodynamic Properties of $Cu_2ZnSn(S_xSe_{1-x})_4$ Pentanary Solid Solution

MOHAMED ISSAM ZIANE,[1,7] DJAMEL OUADJAOUT,[1] MEFTAH TABLAOUI,[1] RACHIDA NOURI,[2] WAFIA ZERMANE,[3] ABDELKADER DJELLOUL,[1] HAMZA BENNACER,[4] ABDERRAHMANE MOKRANI,[1] MOUFDI HADJAB,[5] and HAMZA ABID[6]

1.—Research Center in Semiconductor Technologies for Energetic (CRTSE), 02 Bd Frantz Fanon, BP. 140, Algiers, Algeria. 2.—Laboratory of Thin Film and Interface, Department of Physics, Faculty of Exact Sciences, Brothers Mentouri, Constantine 1 University, Ain El Bye, Constantine, Algeria. 3.—Department of Physics, Faculty of Sciences, Saad DAHLEB University of Blida, 09000 Blida, Algeria. 4.—University of M'sila, M'sila, Algeria. 5.—Thin Films Development and Applications Unit UDCMA, Setif–Research Center in Industrial Technologies CRTI, P.O. Box 64, 16014 Cheraga, Algiers, Algeria. 6.—Applied Materials Laboratory, Research Center, University Djillali Liabes of Sidi Bel Abbes, 22000 Sidi Bel Abbès, Algeria. 7.—e-mail: issam1308@yahoo.fr

This paper is dedicated to the ab initio study of the structural and thermodynamic properties of $Cu_2ZnSn(S_xSe_{1-x})_4$ bulk alloys. The calculations are conducted using full-potential linear-augmented-plane-wave plus local-orbital (FP-LAPW + lo) method within the revised generalized gradient approximation of Perdew–Burke–Ernzerhof (GGAPBEsol). This method is used to find more valuable equilibrium structural parameters than the simplest approximations of PBE and local density approximation (LDA). The obtained structural properties appear to be affected by the relaxation effect, and all alloys are thermodynamically favorable to the process according to the enthalpy of formation calculations. We find here a nonlinear dependence of lattice parameters a and c with respectively a small downward bowing parameter b of + 0.09 Å and + 0.19 Å for relaxed structures. The thermodynamic quantities, namely the entropy, the constant volume, the pressure heat capacity (Cv and Cp) and Debye temperature, are computed for different S/(S + Se) atomic ratios by varying temperature from 0 K to 1000 K. These quantities are successfully obtained by using the combined approach of FP-LAPW and a quasi-harmonic model. Overall, there is good agreement between our calculated quantities and other results.

Key words: DFT, CZTSSe, stannite, lattice parameters, Debye temperature

INTRODUCTION

One of the important objectives of materials science is to study the electronic structure which can be determined either by experimental means or by numerical simulations. Indeed, in complement with the experimental observations, the last decades have witnessed the appearance of ab initio numerical methods which make it possible to study the ground-state properties of the materials by solving the equations of quantum mechanics by appealing to the lowest possible number of adjustable parameters. Ab initio methods have yielded several breakthroughs in the understanding of the underlying physics in such systems. Density functional theory (DFT) is likely the most commonly ab initio approach and is well implemented in many different codes. It succeeds in describing structural

(Received November 12, 2018; accepted July 27, 2019)

Published online: 12 August 2019

and electronic properties for a wide class of materials.

Semiconductor alloys are extensively used for engineering material properties through tuning the alloy composition. From a practical point of view, chalcogenide materials present a good choice to the scientific community due to their great structural diversity as well as to the ability to modulate their physical properties by acting on the elemental composition. The main members of this family materials are the copper-zinc-tin-sulfide (CZTS) and copper-zinc-tin-selenide (CZTSe). These quaternaries are semiconductor materials of group I_2–II–IV–VI_4. The varied physical properties of this group suggest numerous applications, notably for solar cells[1] because of their earth-abundant elements, low-cost, and low toxicity.[2–4] CZTS and CZTSe have been reported to crystallize in tetragonal kesterite (I-4) or a stannite (I-42 m) structure which depends on the thermodynamic conditions and the synthesis method. The difference between kesterite and stannite structures is in the different distribution of zinc and copper elements, while the placement of other atoms remains unchanged.

The mixed chalcogenide $Cu_2ZnSn(S_xSe_{1-x})_4$ belongs also to the I_2–II–IV–VI_4 quaternary material system with a similar structure to that of quaternary CZTS and CZTSe. In 2012, Ou et al.[2] synthesized $Cu_2ZnSn(S_xSe_{1-x})_4$ in nanocrystals by a "hot injection" protocol, in that the metal stearates dissolve in oleylamine and are injected into a hot solution of anion precursors. The results reported by Ou et al.[2] for $Cu_2ZnSn(S_xSe_{1-x})_4$ nanocrystals with x values of 1, 0.7, 0.5, 0.3 and 0 compositions reveal that all materials exhibit a stannite structure with I-42 m as the space group. In 2014, CZTSSe alloys (x = 0, 0.2, 0.5, 0.8, 1) were also successfully grown by Nagaoka et al.[3] with the melting growth method. The stoichiometric of all elements are charged into a quartz ampule and heated up to 1100°C in a vertical furnace. Powder x-ray diffraction (XRD) indicates that the polycrystalline CZTSSe alloys crystallize in the tetragonal-scalenoidal structure with a space group of I-42 m.

In this work, we shall perform ab initio calculations of structural and thermodynamic properties of the stannite $Cu_2ZnSn(S_xSe_{1-x})_4$ quinary alloys for nine compositions (x = 0, 0.125, 0.25, 0.375, 0.5, 0.625, 0.75, 0.875 and 1). This study aims at applying one of the advanced computational methods to gain a deeper insight into sulfur substitution and extract the advantages that one can draw from its mixture with selenium. Based on density functional theory (DFT) method within WIEN2K computational code,[5] the lattices parameters, bulk modulus, enthalpy of formation per atom and other thermodynamic quantities have been carefully calculated and discussed.

Before arriving at interpretations and calculation results, it is necessary to recall the approximations and the method used in this study. After having laid down a certain number of definitions, we will make a quick overview of the crystalline configuration and structural relaxation for each material. This latter effect, which may seem weak in the case of non-ordered alloys, cannot be neglected in view of systems we are led to study. This article is organized as follows. In "Calculation Methodology" section, we provide a theoretical overview of the computational method. Results and discussions will be presented in "Results and Discussions" section, and a summary of our work is given in "Conclusion" section.

CALCULATION METHODOLOGY

Ab initio method is used here to predict the material properties by solving the equations of quantum mechanics without using any adjustable variables. The full-potential linear-augmented-plane-wave plus local-orbital (FP-LAPW + lo) method[6] based on DFT is used in this paper to predict the structural and thermodynamic properties of $Cu_2ZnSn(S_xSe_{1-x})_4$ quinary alloys. Additionally, we use for the exchange–correlation functional the revised Perdew-Burcke-Ernzerhof (PBEsol) parameterization of the generalized gradient approximation (GGA) functional[7] in order to give a good structural optimization. We limit ourselves to a fully relativistic core and scalar relativistic valence computation and without polarized spin. In WIEN2K computational code, core electrons are assumed to not interact. Separating energy of −6.0Ry is used to separate the core from valence states. This value specifies the energy below which its states are treated as core states. Rmt*Kmax determines matrix size (convergence), where Kmax is the plane wave cutoff, and Rmt is the smallest of all atomic sphere radii. RKmax is fixed at 8. In the present work, we use the atomic sphere radius (muffin-tin radius) of 2.050 a.u., 2.050 a.u., 2.40 a.u., 2.00 a.u. and 2.10 a.u. for Zn, Cu, Sn, S and Se atoms, respectively. The maximum l value for partial waves used inside atomic spheres ($l$max) and for computation of non-muffin-tin matrix elements (lnsmax) are fixed at 10 and 4, respectively. A value of 12 is chosen for the maximum magnitude (Gmax) of the largest vector in charge density Fourier expansion. The results-based 64 atoms in the primitive structure are given for 300 k-point meshes equivalent to a $6 \times 6 \times 6$ grid in the irreductible Brillouin zone.

RESULTS AND DISCUSSIONS

Stable Configuration and Structural Relaxation

Crystallographically speaking, CZTS and CZTSe are described with a lower symmetry in a kesterite structure (I-4).[8] These two materials can be also crystallized in the stannite structure with space group I-42 m. In this stannite structure, a random

onsite distribution of Cu and Zn (50/50) occurs in the Cu/Zn layer leading to a higher symmetry.[9] This class of structure is tetrahedrally coordinated and is no-centro symmetric and anisotropic-uniaxial material (along the *z*-axis). According to the experimental results from Nagaoka et al.[3] and He et al.,[10] the quinary alloy $Cu_2ZnSn(S_xSe_{1-x})_4$ exhibits a stannite structure with a body-centered Bravais lattice. Treating theoretically the alloy (solid solution) for all x composition is a delicate task. The major difficulty is to reproduce the crystal in the best way ever and to know the substitution sites and their symmetries. In this study, we perform FP-LAPW calculation to predict the structural and thermodynamic properties of $Cu_2ZnSn(S_xSe_{1-x})_4$ alloys. By respecting the octet rule, the properties are calculated and interpreted for different S/(S + Se) atomic ratios, ranging from 0 to 1 with a step of 0.125. When the ratio is equal to zero or one, the material is stoichiometric as for CZTSe and CZTS, respectively. For this purpose, and based on the super-cell concept, we created a tetragonal crystal with stannite structure which contains a sufficient number of atoms to mimic as closely as possible the considered materials. The calculations are performed on a super-cell of $2 \times 2 \times 2$ with 128 atoms in the conventional structure. In this super-cell, sulfur (S) and selenium (Se) occupy 32 distinct lattice sites. The compositions correspond to 12.5% (4S), 25% (8S), 37.5% (12S), 50% (16S), 62.5% (20S), 75% (24S) and 87.5% (28S) deviations of stoichiometry. Figure 1 shows an example of a stannite super-cell for $Cu_{16}Zn_8Sn_8S_{16}Se_{16}$.

Before studying the physical properties of alloys of which we are interested in this paper, we have to go through three essential steps: stable configuration, structural relaxation and geometric optimization. Our constructed super-cell consists of six possible substitution sites in which the S and Se anions are randomly distributed in their internal sublattice. Table I shows the atomic positions with their fractional coordinates, their multiplicity and their Wyckoff positions. For all alloys, 62 64 atoms-based super-cells with different random arrangements of S are constructed.

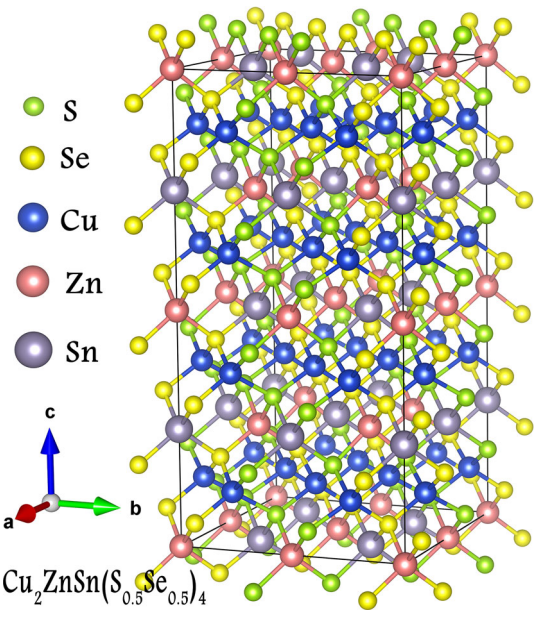

Fig. 1. Conventional stannite super-cell for $Cu_{16}Zn_8Sn_8S_{16}Se_{16}$.

The most stable configuration of $Cu_2ZnSn(S_xSe_{1-x})_4$ quinary alloy for different concentration is defined by calculating the total energy difference ΔE between the mixing energy predicted from the pure quaternary energies and considered as reference energy, and the minimal energy calculated with GGAPBEsol for each configuration.

$$\Delta E = E^{\mathrm{mix}}_{\mathrm{CZTSSe}} - E^{\mathrm{min}}_{\mathrm{CZTSSe}} \tag{1}$$

$E^{\mathrm{mix}}_{\mathrm{CZTSSe}}$ corresponds to the mixing energy and $E^{\mathrm{min}}_{\mathrm{CZTSSe}}$ is the minimal energy obtaind with GGAPBEsol. The mixing energy for the quinary alloys with different x compositions can be derived from pure quaternary energies by the following equation:

$$E^{\mathrm{mix}}_{\mathrm{Cu_2ZnSn(S_xSe_{1-x})_4}} = x \cdot E^{\mathrm{min}}_{\mathrm{Cu_2ZnSnS_4}} + (1-x) \cdot E^{\mathrm{min}}_{\mathrm{Cu_2ZnSnSe_4}} \tag{2}$$

Here, $E^{\mathrm{min}}_{\mathrm{Cu_2ZnSnS_4}}$ and $E^{\mathrm{min}}_{\mathrm{Cu_2ZnSnSe_4}}$ represent the minimum energies from calculations performed with GGAPBEsol for pure quaternary alloys CZTS and CZTSe, respectively. The mixing energy of $Cu_2ZnSn(S_xSe_{1-x})_4$ for x composition is $E^{\mathrm{mix}}_{\mathrm{Cu_2ZnSn(S_xSe_{1-x})_4}}$.

Table II reports an example of the possible combinations for the crystal structures of the quinary alloys with 25% and 75% of sulfur and selenium, respectively. If we take the quinary alloy $Cu_2ZnSn(S_{0.25}Se_{0.75})_4$ as an example, the mixing energy for this concentration can be defined trough the following equation:

$$E^{\mathrm{mix}}_{\mathrm{Cu_2ZnSn(S_{0.25}Se_{0.75})_4}} = (0.25)E^{\mathrm{min}}_{\mathrm{Cu_2ZnSnS_4}} + (0.75)E^{\mathrm{min}}_{\mathrm{Cu_2ZnSnSe_4}} \tag{3}$$

The calculated mixing energy for $Cu_2ZnSn(S_{0.25}Se_{0.75})_4$ is equal to −303406, 4308414625 Ry. From Table II and according to energy difference (ΔE), the sixth configuration presents the lowest minimum energy over the other configurations and is considered as the most stable one.

As aforementioned, after determining the stable configurations, the atom positions are fully relaxed for all structures. The relaxation consists of finding the groundstate relaxed geometry of the system. During relaxation, certain correlations between atomic positions set in, interatomic distances adjust to reasonable values, and unfavorable interactions are avoided. The resulting structures for all compositions are the initials for all further steps.

Table I. Cationic and anionic atomic positions with their fractional coordinates, their multiplicity and Wyckoff positions as presented in our structure file

Atomic positions label	Atom occupancies	Fractional coordinates			Multiplicity	Wyckoff positions
		x	*y*	*z*		
Position 1	Zn	0.000	0.000	0.000	1	2a
Position 2	Zn	0.500	0.000	0.000	2	2a
Position 3	Zn	0.500	0.500	0.000	1	2a
Position 4	Zn	0.750	0.250	0.250	4	2a
Position 5	Sn	0.750	0.750	0.000	4	2b
Position 6	Sn	0.000	0.500	0.250	2	2b
Position 7	Sn	0.500	0.500	0.250	2	2b
Position 8	Cu	0.750	0.000	0.375	8	4d
Position 9	Cu	0.750	0.500	0.375	8	4d
Position 10	S/Se	0.125	0.125	0.0625	4	8g
Position 11	S/Se	0.125	0.625	0.0625	8	8g
Position 12	S/Se	0.625	0.625	0.0625	4	8g
Position 13	S/Se	0.375	0.375	0.3125	4	8g
Position 14	S/Se	0.375	0.875	0.3125	8	8g
Position 15	S/Se	0.875	0.875	0.3125	4	8g

Table II. Atomic positions and the eight possible configurations corresponding to 25% of sulfur and 75% of selenium in the form of $Cu_2ZnSn(S_{0.25}Se_{0.75})_4$ alloys

Configurations for $x = 0.25$	Atomic positions of S and Se in our crystalline structure						Minimal energy E^{min} (Ry)	ΔE (Ry)
	POS 10	POS 11	POS 12	POS 13	POS 14	POS 15		
1st structure	Se	S	Se	Se	Se	Se	−303406.22355059	−0.2072908725
2nd structure	Se	Se	Se	Se	S	Se	−303406.22254785	−0.2082936125
3rd structure	S	Se	S	Se	Se	Se	−303406.22355063	−0.2072908325
4th structure	S	Se	Se	S	Se	Se	−303406.22388522	−0.2069562425
5th structure	S	Se	Se	Se	Se	S	−303406.2256791	−0.2051623625
6th structure	Se	Se	S	S	Se	Se	−303406.22567927	−0.2051621925
7th structure	Se	Se	S	Se	Se	S	−303406.22388531	−0.2069561525
8th structure	Se	Se	Se	S	Se	S	−303406.22254781	−0.2082936525

The calculated minimal energies with GGAPBEsol for each configuration are gathered here. The total energy differences (ΔE) are also reported. The sixth configuration is underlined because it presents minimal energy over the others and is considered to be the most stable configuration.

The process of optimization is initiated by using the existing geometries reported by Nagaoka et al.[3] For the other compositions for which the experimental values are not available, we optimize the structures by injecting as input parameter the estimated values for lattice parameters calculated with Vegard's law.[11]

$$\begin{cases} a_{Cu_2ZnSn(S_xSe_{1-x})_4} = xa_{Cu_2ZnSnS_4} + (1-x)a_{Cu_2ZnSnSe_4} \\ c_{Cu_2ZnSn(S_xSe_{1-x})_4} = xc_{Cu_2ZnSnS_4} + (1-x)c_{Cu_2ZnSnSe_4} \end{cases} \quad (4)$$

where $a_{Cu2ZnSnS4}$, $c_{Cu2ZnSnS4}$ and $a_{Cu2ZnSnSe4}$, $c_{Cu2ZnSnSe4}$ represent the lattice parameters a and c in the stannite structure of pure Cu_2ZnSnS_4 and $Cu_2ZnSnSe_4$, respectively. The lattice parameters of the alloy $Cu_2ZnSn(S_xSe_{1-x})_4$ for the x composition are $a_{Cu2ZnSn(SxSe1-x)4}$, $c_{Cu2ZnSn(SxSe1-x)4}$.

Structural Optimization

The first step in dealing with the tasks we have just presented in the introduction of our present paper is the optimization of lattice structures. The optimization allows us to find a true fundamental state of the crystal. The theoretical ground-state energy E (V) as a function of the unit cell volume V is calculated with the revised Perdew–Burke–Ernzerhof GGA approximation (GGAPBEsol). The

minimum of the function E (V) corresponds to the optimal value of lattice parameters (see Fig. 2). The 0-K equilibrium properties for all materials such as the lattice parameters and the isothermal bulk modulus reported in Table III are determined by fitting the calculated E (V) with respect to the volume and the pressure to the Murnaghan equation of state.[12] In view of these first results, we can say that the approximation GGAPBEsol is satisfactory. Although absolute errors remain significant, all density functional theory (DFT) methods give comparable results. There are not enough experimental or theoretical results for all x compositions. Comparing our calculated lattice parameter a with experimental data of Nagaoka et al.[3] and He et al.,[10] we find that our results for both un-relaxed and relaxed ones obtained by GGAPBEsol are so far very conclusive, which undoubtedly validates this supercell for our quinary alloys. The same qualitative agreement is noticed with regard to the theoretical result of Zamulko et al.[13] computed with GGAPBEsol based on projector augmented wave (PAW) method as implemented in the Vienna ab initio simulation package (VASP).[15]

The accuracy of the calculations is less than 1.8% error for a and c compared to experimental results. At this point, it should be emphasized that, due to the difference in the occupation of atomic orbitals,

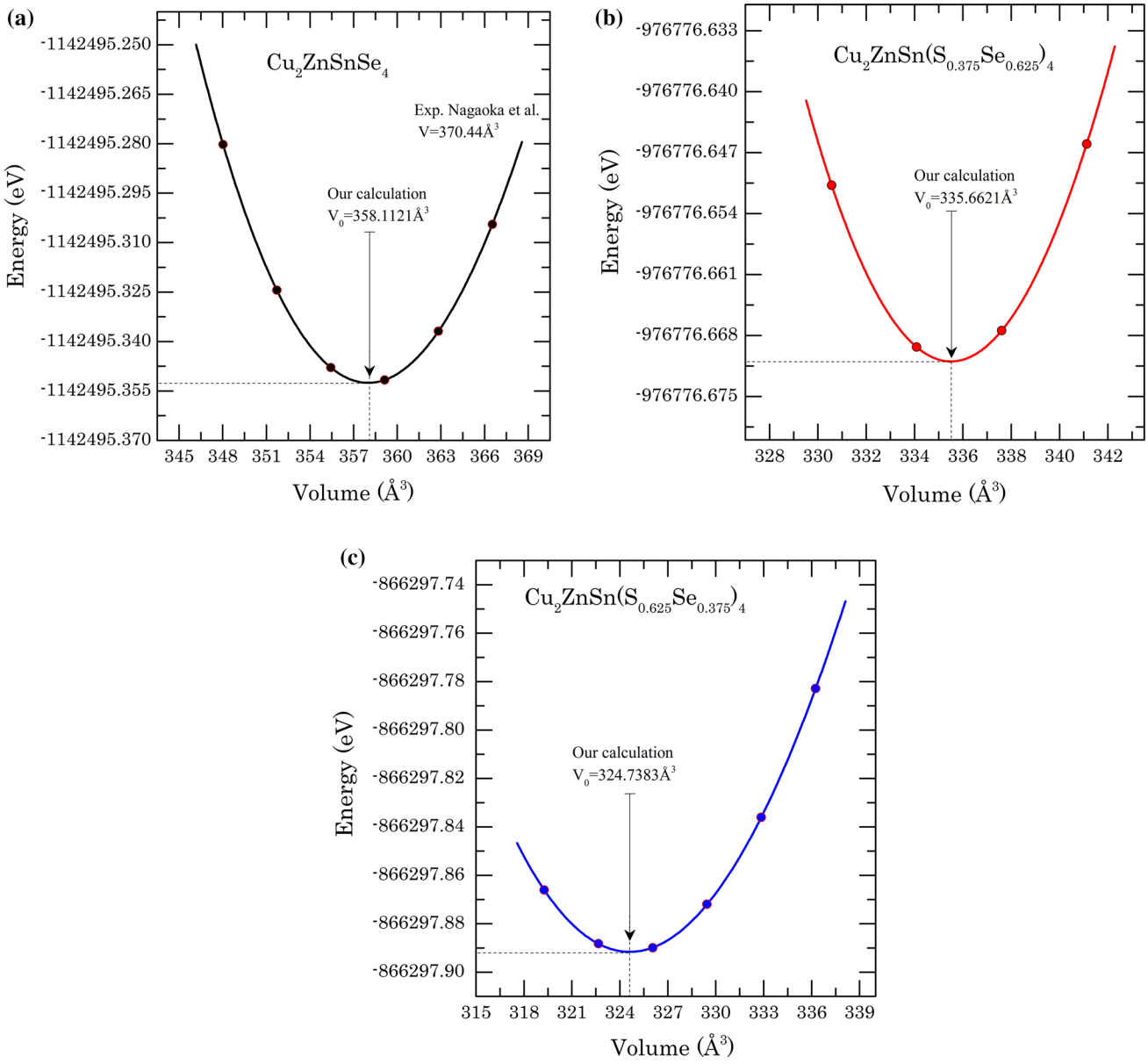

Fig. 2. Zero Kelvin total energy as volume curves for (a) CZTSe, (b) $CZTS_{0.375}Se_{0.625}$ and (c) $CZTS_{0.625}Se_{0.375}$. Ball symbols are direct calculation results by GGAPBEsol, and solid lines are fitted E–V curves according to the Murnaghan EOS. We added the experimental volume for CZTSe of Nagaoka et al.[3] in comparison with our calculation.

Table III. Optimized primitive cell volume, lattices parameters (*a*) and (c), the *c*/*a* ratio, bulk modulus (*B*) and the first derivative of bulk modulus (*B*′) at 0 K

Compositions	*a* (Å)	*c* (Å)	*c*/*a*	*B* (GPa)	*B*′
Se_4					
GGAPBEsol	5.645 (5.641)	11.516 (11.254)	2.040 (1.995)	76.568 (79.022)	3.981 (4.294)
Exp. results	**5.692[a] 5.696[b]**	**11.434[a] 11.385[b]**	**2.008[a]1.998[b]**	–	–
Other calc.	5.661[c]	11.318[c]	1.999[c]	–	–
$(S_{0.125}Se_{0.875})_4$					
GGAPBEsol	5.588 (5.578)	11.393 (11.135)	2.038 (1.996)	83.922 (85.976)	4.255 (3.759)
Exp. results	–	–	–	–	–
$(S_{0.25}Se_{0.75})_4$					
GGAPBEsol	5.562 (5.548)	11.335 (11.077)	2.038 (1.9965)	84.866 (87.436)	4.889 (4.838)
Exp. results	–	–	–	–	–
Other calc.	5.594[c]	11.180[c]	1.998[c]	–	–
$(S_{0.375}Se_{0.625})_4$					
GGAPBEsol	5.537 (5.519)	11.271 (11.020)	2.035 (1.9969)	85.210 (87.257)	4.078 (3.595)
Exp. results	–	–	–	–	–
$(S_{0.5}Se_{0.5})_4$					
GGAPBEsol	5.507 (5.488)	11.214 (10.966)	2.036 (1.998)	84.602 (87.944)	3.512 (4.271)
Exp. results	**5.605[a] 5.563[b]**	**11.256[a] 11.096[b]**	**2.008[a]1.994[b]**	–	–
Other calc.	5.513[c]	11.032[c]	2.001[c]	–	–
$(S_{0.625}Se_{0.375})_4$					
GGAPBEsol	5.476 (5.457)	11.156 (10.905)	2.037 (1.9983)	87.180 (89.714)	4.586 (5.145)
Exp. results	–	–	–	–	–
$(S_{0.75}Se_{0.25})_4$					
GGAPBEsol	5.440 (5.426)	11.070 (10.844)	2.034 (1.9984)	86.966 (90.018)	4.116 (4.557)
Exp. results	–	–	–	–	–
Other calc.	5.440[c]	10.897[c]	2.003[c]	–	–
$(S_{0.875}Se_{0.125})_4$					
GGAPBEsol	5.405 (5.392)	11.012 (10.781)	2.037 (1.9994)	89.165 (91.252)	4.353 (4.35)
Exp. results	–	–	–	–	–
S_4					
GGAPBEsol	5.402 (5.388)	10.983 (10.778)	2.033 (2.0004)	84.820 (86.073)	4.203 (4.373)
Exp. results	**5.443[a] 5.411[b] 5.455[d]**	**10.879[a] 10.832[b] 10.880[d]**	**1.998[a]2.001[b] 1.9945[d]**	**83.6[d]** –	– –
Other calc.	5.374[c]	10.751[c]	2.000[c]	–	–

Bold indicates the experimental values.
The results obtained for the relaxed structures are in parentheses.
[a]Ref. 3.
[b]Ref. 10 for $x = 0.49$.
[c]Ref. 13 with GGAPBESol (PAW-VASP).
[d]Ref. 14.

the substitution of the sulfur atom with selenium would lead to shrinkage of the unit cell.

For more details, we plot also the calculated difference in percent between our calculated lattice parameters *a* and *c* and the experimental data of He et al.[10] and Nagaoka et al.[3] for $x = 0$, 0.5 and 1.

$$\left.\begin{aligned}\Delta a &= \frac{a_{\mathrm{Cal}} - a_{\mathrm{Exp}}}{a_{\mathrm{Exp}}} 100\% \\ \Delta c &= \frac{c_{\mathrm{Cal}} - c_{\mathrm{Exp}}}{c_{\mathrm{Exp}}} 100\%\end{aligned}\right\} \quad (5)$$

The difference in lattice parameter *a* presented in Fig. 3 indicates that our calculations for both un-relaxed and relaxed structures are underestimated with respect to the experimental values. Our calculated values are closer to the results of He et al.[10] than those of Nagaoka et al.[3] for $x = 0.5$ and 1, and a slight difference from experimental results is noted for $x = 0$. In the case of lattice parameter *c* (Fig. 4), in the majority, the un-relaxed and relaxed structures are respectively overestimated and underestimated with respect to the experimental values of Nagaoka et al. and He et al.

Figures 5 and 6 show respectively the variations of lattice constants *a* and *c* for $Cu_2ZnSn(S_xSe_{1-x})_4$ as a function of *x* compositions, led by structural calculations that allow us to observe a nonlinear dependence of the lattice parameters *a* and *c*. There is a decrease in lattice parameters *a* and *c* when we substitute Se with S which is confirmed by the experimental results of Nagaoka et al.[3] and He et al.[10] The results show that the variation in lattice parameters *a* and *c* as a function of sulfur content in

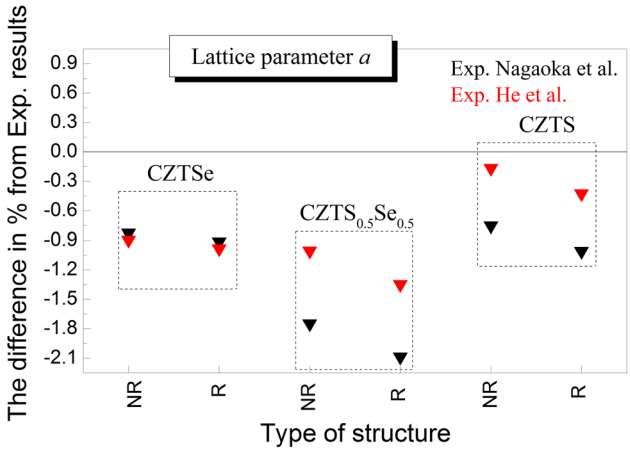

Fig. 3. Plot of the difference between our calculated lattice parameter *a* and the experimental data versus composition for $x = 0$, 0.5 and 1. In this figure, NR and R designate an un-relaxed and relaxed structure, respectively. The experimental values for *a* are taken from Nagaoka et al.[3] and He et al.,[10] and only data was used from the cited reference. The difference from these experimental data is presented in black and red color, respectively (Color figure online).

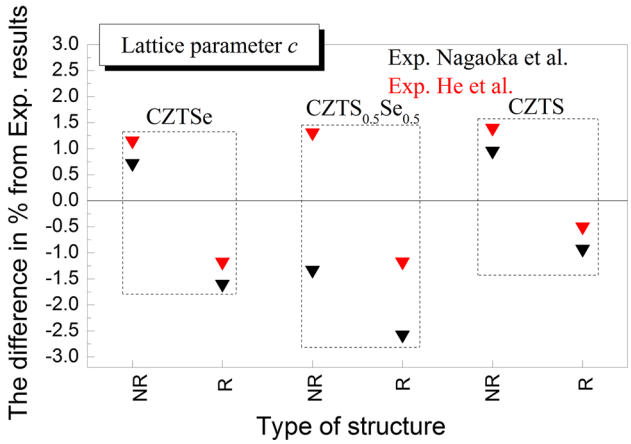

Fig. 4. Plot of the difference between our calculated lattice parameter c and the experimental data versus *x* composition and structure. In this figure, NR and R designate an un-relaxed and relaxed structure, respectively. The experimental values for *a* are taken from Nagaoka et al.[3] and He et al.,[10] and only data was used from the cited reference. The difference from these experimental data is presented in black and red color, respectively (Color figure online).

$Cu_2ZnSn(S_xSe_{1-x})_4$ exhibits a negative deviation from the linear variation of Vegard's law. This deviation is characterized by bowing parameter *b* computed by an appropriate fitting of the nonlinear variation of the calculated lattice parameters. For the relaxed structures (fundamental state), we notice a bowing parameter *b* of +0.099 for lattice parameter *a* and +0.193 Å for *c*. The bulk modulus behaves like the opposite of the lattice parameter, and a large positive deviation is noted. Our results for *a*, *c*, c/a and bulk modulus *B* for both un-relaxed and relaxed structures can be estimated by the

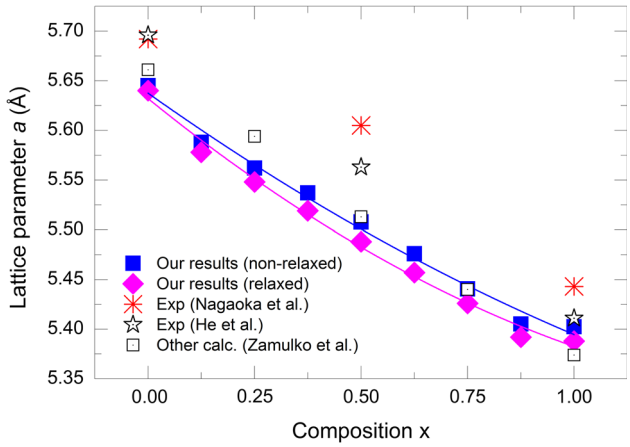

Fig. 5. Lattice parameter *a* as a function of *x* for $Cu_2ZnSn(S_xSe_{1-x})_4$ alloys for both un-relaxed and relaxed structures together with the polynomial fit for determining the slope of the curve in an equation. We added other experimental results for some *x* compositions. Only data from the cited Refs. 3 and 10 was used.

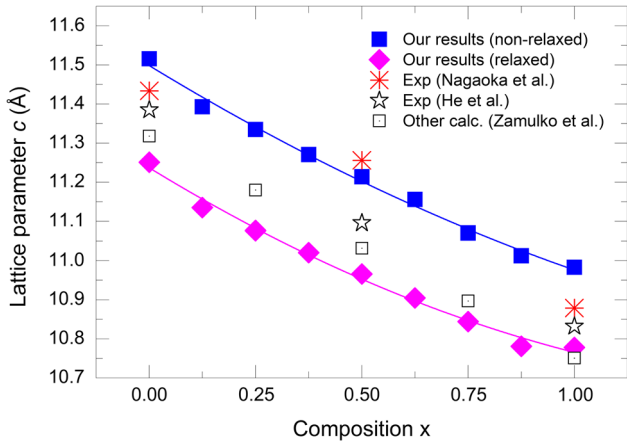

Fig. 6. Lattice parameter *c* as a function of *x* for $Cu_2ZnSn(S_xSe_{1-x})_4$ alloys for both un-relaxed and relaxed structures. Only data from the cited Refs. 3 and 10 was used.

following quadratic polynomial functions presented in Table IV.

The enthalpy of formation per atom $\Delta_f H$ for our materials is given by subtracting the total energy $Emin\_{CZTSSe}$ of the CZTSSe in this equilibrium crystal structure from the sum energies of constituent elements with respect to stoichiometric amounts of Cu, Zn, Sn, S and Se constituents. Our calculated values based on GGAPBEsol approximation for $\Delta_f H$ are predicted according to the following relations:

$$\Delta_f \mathrm{H}(Cu_2ZnSnS_4) = \left[E^{\min}_{Cu_2ZnSnS_4} - \left[2E^{\min}_{Cu} + E^{\min}_{Zn} + E^{\min}_{Sn} + 4E^{\min}_{S}\right]\right]/n \quad (6)$$

$$\Delta_f \mathrm{H}(Cu_2ZnSnSe_4) = \left[E^{\min}_{Cu_2ZnSnSe_4} - \left[2E^{\min}_{Cu} + E^{\min}_{Zn} + E^{\min}_{Sn} + 4E^{\min}_{Se}\right]\right]/n \quad (7)$$

Table IV. The quadratic polynomial functions for predicted *a*, *c*, *c*/*a* and bulk modulus B for both un-relaxed and relaxed structures

	Un-relaxed structure	Relaxed structure
Lattice parameter a (Å)	$5.637 - 0.304x + 0.061x^2$	$5.632 - 0.348x + 0.099x^2$
Lattice parameter c (Å)	$11.498 - 0.663x + 0.140x^2$	$11.237 - 0.665x + 0.193x^2$
c/a ratio	$2.039 - 0.008x + 0.003x^2$	$1.995 + 0.004x + 0.000096x^2$
Bulk modulus B (GPa)	$78.455 - 25.805 - 18.484x^2$	$80.474 + 29.312x - 22.425x^2$

The values of the bowing parameter of a and c are equal to +0.099 Å and +0.193 Å, respectively, for relaxed CZTSSe alloy.

Table V. The estimated enthalpies of formation per atom for $Cu_2ZnSn(S_xSe_{1-x})_4$ alloys calculated with GGA-PBEsol for different *x* composition, and compared with other available results

	$\Delta_f H$ at T = 0 K (in eV/atom)		
	Our results		
Compositions	Un-relaxed	Relaxed	Other results
$Cu_2ZnSnSe_4$	−4.028596	−4.088872	−3.225,[17] −4.238,[18] −3.268[18]
$Cu_2ZnSn(S_{0.125}Se_{0.875})_4$	−4.072957	−4.143319	–
$Cu_2ZnSn(S_{0.25}Se_{0.75})_4$	−4.135202	−4.210201	−4.302,[18] −3.368[18]
$Cu_2ZnSn(S_{0.375}Se_{0.625})_4$	−4.199127	−4.276912	–
$Cu_2ZnSn(S_{0.5}Se_{0.5})_4$	−4.265744	−4.344214	–
$Cu_2ZnSn(S_{0.625}Se_{0.375})_4$	−4.336031	−4.411718	–
$Cu_2ZnSn(S_{0.75}Se_{0.25})_4$	−4.404868	−4.480819	–
$Cu_2ZnSn(S_{0.875}Se_{0.125})_4$	−4.481725	−4.542364	–
Cu_2ZnSnS_4	−4.639617	−4.687809	−4.21 ± 0.003,[19] −1.2 ± 0.13,[16] −3.7301,[17] −4.596,[18] −3.758,[18] −4.572,[20]

The enthalpy of formation energies given here for the pure compounds are for 64-atom super-cells. The experimental results of Baryshev et al.[16] in this table refer to $Cu_{1.9}Zn_{1.5}Sn_{0.8}S_4$.

$$\Delta_f \mathrm{H}(\mathrm{Cu_2ZnSn(S_xSe_{1-x})_4} = \left[E^{\min}_{\mathrm{Cu_2ZnSn(S_xSe_{1-x})_4}} - \left[2E^{\min}_{\mathrm{Cu}} + E^{\min}_{\mathrm{Zn}} + E^{\min}_{\mathrm{Sn}} + 4(xE^{\min}_{\mathrm{S}} + (1-x)E^{\min}_{\mathrm{Se}})\right]\right]/n \quad (8)$$

Here, n is the number of atoms. All minimum total energies are expressed per atom at 0 K and 0 Pa and obtained with the same XC functional, RmtK-max and same K points. The enthalpy of formation per atom for our pure compounds and alloys is calculated at a given stoichiometry for both structures and is summarized in Table V. The table shows that the agreement between our calculated enthalpy of formation for 64 atoms and the available theoretical data is good with a small discrepancy. This discrepancy can be attributed to the cation ordering. Baryshev et al.[16] predicted quite different enthalpy of formation compared to our and other results. It is worth noting that the enthalpy of formation of Baryshev et al. was measured at the composition of Cu, Zn, Sn and S of 1.9:1.5:0.8:1 by sputtering rates measured during ion bombardment. By analyzing the enthalpy of formation results, one can say that the latter is not equal to zero, because the mixing process makes available additional energy levels for the solid solution, and the formation of the solid solution alloys is practically allowed. For instance, in Fig. 7, we present dependence of this quantity with respect to x composition and we can see that the calculated enthalpy of formation per atom $\Delta_f H$ for the quinary alloys $Cu_2ZnSn(S_xSe_{1-x})_4$ experiencing a near-linear increase with an increase in S alloying composition with a difference less than 70 meV.

Thermodynamic Properties

Before going further in understanding the fundamental properties, we introduce the thermodynamic quantities in order to show in more detail the influence of sulfur content in our solid solution. In this study, we use the quasi-harmonic Debye model code gibbs2 developed by Otero-de-la-Roza et al.[21] to

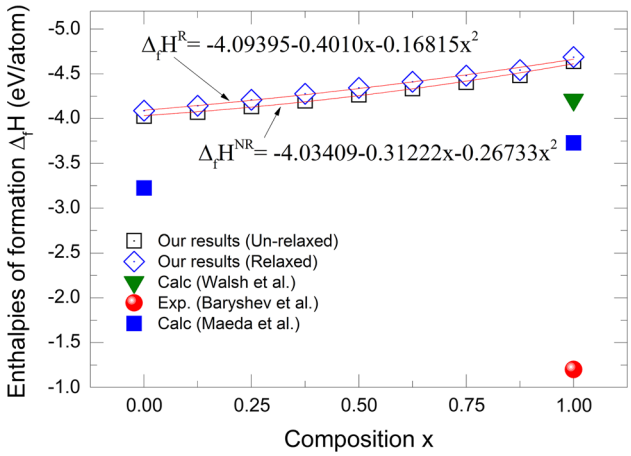

Fig. 7. The dependence of the enthalpies of formation with respect to *x* composition. Only data from the cited Refs. 16, 17 and19 was used.

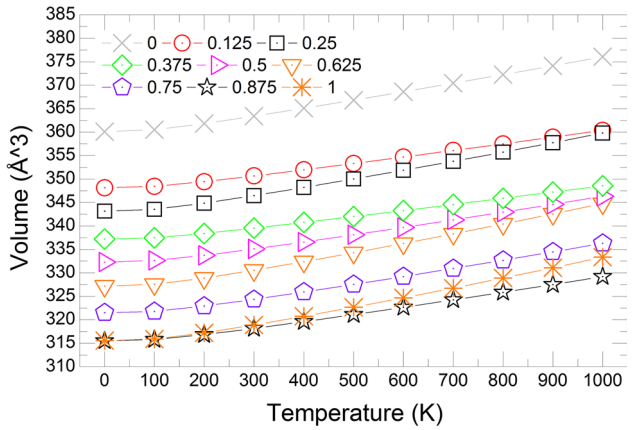

Fig. 8. Volume of $Cu_2ZnSn(S_xSe_{1-x})_4$ for a range of temperatures from 0 K to 1000 K, with zero pressure.

predict the thermodynamic properties for various temperatures at zero pressure. In this code, when the E (V) curve is available, the quasi-harmonic Debye model can be properly applied. The total energy system versus volume theoretical curve obtained from our structural calculations within WIEN2K is used to derive the equilibrium entropy (S), the constant volume and pressure heat capacity (Cv) and (Cp) and Debye temperature. In addition to that, we show also the temperature dependence on the volume (V). The thermodynamic properties of the system are determined by using the non-equilibrium Gibbs energy function represented by the following equation:

$$G^*(V;\ p,\ T) = E(V) + pV + F^*_{\text{vib}}(\Theta(V);T) = F^*(\Theta(V);T) + pV \quad (9)$$

where E (V) is the total energy, pV corresponds to the constant hydrostatic pressure condition, F_{vib} is the vibrational Helmholtz free energy which includes both the vibrational contribution to the internal energy and the entropy S that are strong functions of temperature and Θ (V) is the Debye temperature. For a solid, the thermodynamic functions are determined mostly by the vibrational degrees of freedom of the lattice, since, generally speaking, the electronic degrees of freedom play a noticeable role only for metals at very low temperatures.[22] The vibrational contribution of Helmholtz free energy is given by Ref. 23

$$F_{\text{vib}}(\Theta;\ T) = \frac{9}{8}nk_{\text{B}}\Theta_D + 3nk_{\text{B}}T\ \ln(1-e^{-\Theta_D/T}) - nk_{\text{B}}T\,D(\Theta_D/T) \quad (10)$$

where D is the Debye integral and n is the number of atoms.

The Debye temperature is given by[21]

$$\Theta_D = \frac{\omega_D}{k_{\text{B}}} = \frac{1}{k_{\text{B}}}\left(\frac{6\pi^2 n}{V}\right)^{1/3} v_0 \quad (11)$$

Here, ω_{D} is the Debye frequency. In the quasiharmonic Debye model, Θ_{D} is a function of volume, and the Grüneisen (γ) ratio is

$$\gamma_D = -\frac{\partial \ln \Theta_D}{\partial \ln V} \quad (12)$$

All thermodynamic properties are for relaxed structures. Figure 8 illustrates the dependence of the temperature T on volume V for different x composition. Thermodynamically speaking, the internal configuration parameters and the volume of the material at temperature T is decided by the minimum value of the Helmholtz free energy $F(V, T)$. The increase in temperature can alter the minima of the free energy variation with the volume, and the shift in the minima represents the change in volume with the temperature. As expected, the volume increases with the increasing of temperature T (see Fig. 8).

The thermodynamic quantity, namely, the entropy, is a particularly important property in clarifying the nature of any disorder in a system. The entropy is obtained from this equation defined as

$$S = -3nk_{\text{B}}\ \ln(1-e^{-\Theta_D/T}) + 4nk_{\text{B}}\,D(\Theta_D/T) \quad (13)$$

Thermodynamically speaking, the higher the entropy of the system, the more the microscopic disorder in the alloy increases. The analysis of our entropy results displayed in Fig. 9, shows that the latter for our systems is zero when the temperature of the crystal is equal to zero (0 K) and increases with increasing of temperature T. Also, for the same temperature of 300 K, the decrease of entropy is remarked when x composition in $Cu_2ZnSn(S_xSe_{1-x})_4$ relaxed alloys increases. The results of entropy versus temperature obey the following formulation:

$$S^{0\text{GPa}}_{300\text{K}} = 253.47 - 52.80x + 18.69x^2 \quad (14)$$

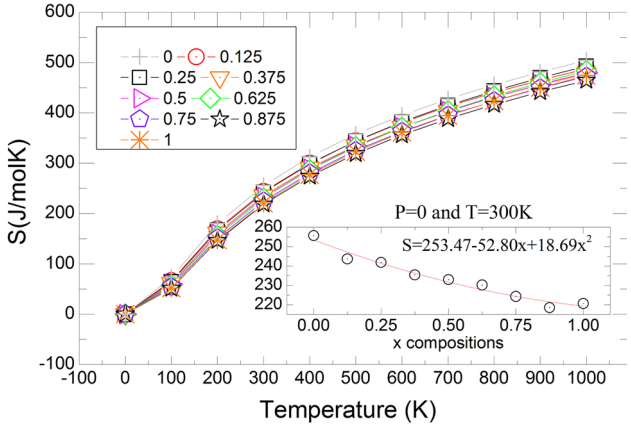

Fig. 9. Calculated entropy of $Cu_2ZnSn(S_xSe_{1-x})_4$ relaxed alloys versus temperature. The inset in the figure is the predicted entropy as a function of x composition at zero pressure and fixed temperature of 300 K.

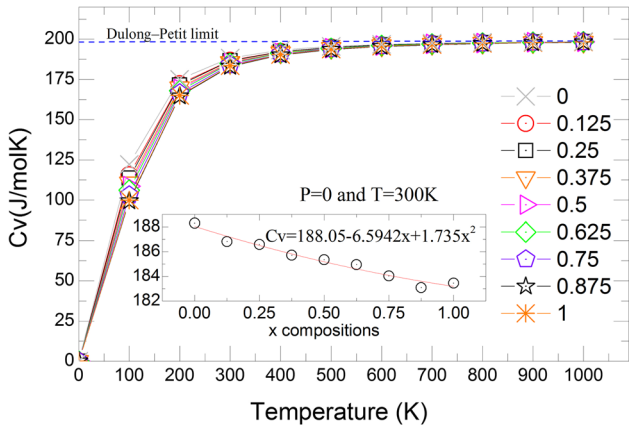

Fig. 10. The calculated temperature dependence on the constant volume heat capacity of $Cu_2ZnSn(S_xSe_{1-x})_4$ relaxed alloys versus temperature. The inset in the figure is the predicted Cv as a function of x composition at zero pressure and fixed 300 K.

The specific heat capacity is a realization of the capability of individual molecules and atoms to absorb and retain thermal energy.[24] For any material, two specific heat capacities, at constant volume and at constant pressure, are defined as the derivatives of the entropy with respect to temperature. The specific heat capacity, at constant volume Cv and constant pressure Cp, are given respectively by

$$C_V = 12nk\, D(\Theta_D/T) - \frac{9nk_B\Theta_D/T}{e^{\Theta_D/T}-1} \qquad (15)$$

$$C_P = C_V(1+\gamma\alpha T) \qquad (16)$$

where α is the thermal expansivity.

The results of the calculation for the specific heat capacity, at constant volume, are computed from Eq. 15 and are plotted in Fig. 10. It is seen from the figure that the calculated variation of Cv for all x compositions is large at low temperatures, and the values practically coincide when the temperature is increased, and reach a plateau around the Dulong-Petit limit. We estimate a value of $\sim$ 198 J/molK for Cv in the limit $T \rightarrow \infty$.

The heat capacity under constant pressure is calculated through the thermodynamic relation.16 The results as a function of temperature in the temperature range from 0 K to 1000 K with no pressure effects are shown in Fig. 11 for different x compositions. With low temperature, the specific heats at constant volume and at constant pressure for any material are almost constant. In this study, (Cp − Cv)/Cp = 0.099% and 0.093% at 50 K are noted for CZTSe and CZTS, respectively. With increasing the temperature, the heat capacity Cp increases very rapidly. When the temperature rises above the Debye temperature (Θ), the Cp increases monotonously with the temperature, contrary to Cv that remains constant. The Debye temperature, in this case, separates two temperature regions, one

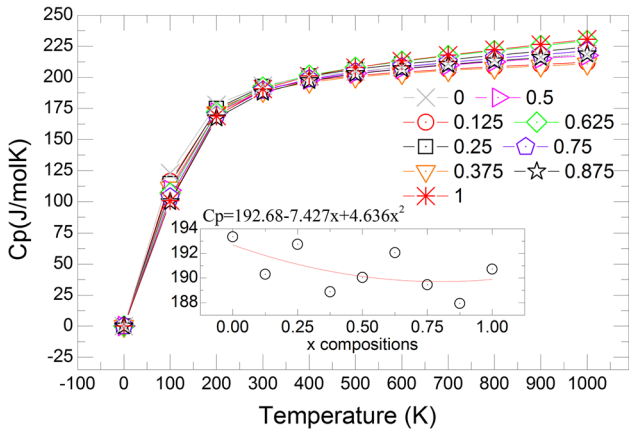

Fig. 11. The calculated temperature dependence on the constant pressure heat capacity of $Cu_2ZnSn(S_xSe_{1-x})_4$ relaxed alloys at different x composition. The inset in the figure is the predicted Cp as a function of x composition at zero pressure and 300 K.

where the atomic vibrations are collective and the other where atoms vibrate independently.

Table VI lists the results for the lattice parameters, bulk modulus, volume and pressure heat capacity and Debye temperature (Θ) values calculated for $Cu_2ZnSn(S_xSe_{1-x})_4$ from quasi-harmonic Debye model code gibbs2 with a temperature fixed at 300 K and zero pressure. The lattice parameters a and c predicted for 300 K are in excellent agreement with both results of Nagaoka et al.[3] and He et al.[10] Also, our calculated value of volume heat capacity Cv (183,45 J/molK) agrees well with 184 J/molK determined experimentally at room temperature by Nagaoka et al.[14] The same agreement is noted for pressure heat capacity Cp. The Debye temperature of the St-type CZTSe is smaller than that of the St-type CZTS at the same temperature because the Debye temperature is in an inverse relationship with the volume. Our estimated Debye temperature for St-CZTS is 392.59 K,

Table VI. The estimated values at 300 K of temperature and zero pressure within quasi-harmonic model of lattices parameters (*a* and *c*), isothermal and adiabatic bulk modulus (B and Bs), equilibrium entropy (S), volume and pressure heat capacity (Cv and Cp) and Debye temperature (Θ) for $Cu_2ZnSn(S_xSe_{1-x})_4$ relaxed alloys at different *x* composition

Compositions	*a* (Å)	*c* (Å)	B (GPa)	Bs (GPa)	S (J/molK)	Cv (J/molK)	Cp (J/molK)	Θ (K)
Se_4	5.6697	11.3111	75.5306	77.5545	255.7013	188.2971	193.3427	325.21
Exp.	**5.692**[a]	**11.434**[a]	–	–	–	–	–	–
	5.696[b]	**11.385**[b]	–	–	–	–	–	–
Other	–	–	–	–	–	–	–	320[c]
$(S_{0.125}Se_{0.875})_4$	5.6018	11.1812	83.3764	84.9335	243.6471	186.825	190.3143	346.8
$(S_{0.25}Se_{0.75})_4$	5.5788	11.1381	82.5705	85.2914	241.8343	186.5875	192.7358	350.18
$(S_{0.375}Se_{0.625})_4$	5.5411	11.0650	84.8619	86.3111	235.4372	185.7117	188.8831	362.43
$(S_{0.5}Se_{0.5})_4$	5.515	11.020	84.2188	86.3538	232.953	185.355	190.0546	367.31
Exp.	**5.605**[a]	**11.256**[a]	–	–	–	–	–	–
	5.563[b]	**11.096**[b]	–	–	–	–	–	–
$(S_{0.625}Se_{0.375})_4$	5.4905	10.9722	83.8247	87.0503	230.2053	184.9507	192.0677	372.8
$(S_{0.75}Se_{0.25})_4$	5.4559	10.9030	85.5185	88.039	224.2837	184.0375	189.4617	384.96
$(S_{0.875}Se_{0.125})_4$	5.4199	10.8366	87.1563	89.4676	218.512	183.0911	187.9465	397.26
S_4	5.4232	10.8486	81.269	84.4913	220.6792	183.4532	190.7271	392.59
Exp.	**5.443**[a]	**10.879**[a]	**83.6**[d]	–	–	**184**[d]	∼ **187**[d]	**302**[d]
	5.411[b]	**10.832**[b]	–	–	–	–	–	–
	5.455[d]	**10.880**[d]	–	–	–	–	–	–
Other	–	–	–	–	–	–	–	400[c]

Bold indicates the experimental values.
[a]Ref. 3.
[b]Ref. 10 for $x = 0.49$.
[c]Ref. 25.
[d]Ref. 16.

greater by about 30% from that of Nagaoka et al. obtained from the measured Cp value below 7 K,[14] and in excellent agreement with that calculated by Adachi et al.[25]

CONCLUSION

Our attention is focused on the mixture of two chalcogens, S and Se, which is the subject of many studies including photovoltaic applications. This investigation is categorized as structural and thermodynamic properties the bulk $Cu_2ZnSn(S_xSe_{1-x})_4$ alloys for different S/(S + Se) atomic ratios, ranging from 0 to 1 with a step of 0.125. We are able to investigate in more detail and for different S composition the lattices parameters, isothermal bulk modulus, enthalpy of formation energy, as well as the thermodynamic quantities deduced from the quasi-harmonic Debye model, namely the entropy, constant volume and pressure heat capacity, and Debye temperature. As a result, the substitution of selenium by sulfur usually leads to a reduction of the lattice parameters because of the small size of the sulfur atoms. The predicted mixing enthalpy is negative (exothermic) for our stannite-based structure, implying that the alloy formation is a thermodynamically favorable process. The effects of structural relaxation are accounted for in our calculations through the mini-program. A significant improvement is noted for these lattices parameters when they are determined at 300 K. The contribution of temperature is fundamental to thermodynamic measurements. The entropy, constant volume and pressure heat capacity, and Debye temperature are computed at a different range of temperatures from 0 K to 1000 K, with zero pressure. No other experimental or theoretical results are found for quinary alloys, and the calculations for parent compounds exhibit an excellent agreement with the data reported by Adachi et al.[25] and Nagaoka et al.[14] This prospective work highlights the different aspects of chalcogenide materials. It will undoubtedly allow predictive calculations of the electronic and optical properties by means of the structural parameters studied here. We can say that the numerical simulation for the study and understanding of physical phenomena is a complementary approach to experimental studies. Finally, we expect that the results of the present work should invoke further experimental and theoretical investigations for these alloys.

ACKNOWLEDGMENTS

The authors would like to thanks the Directorate General for Scientific Research and Technological Development (DGRSDT/MESRS) of Algeria. The authors gratefully acknowledge Prof. Tarik Ouahrani from Tlemcen University and Sajad Ahmad Dar from Govt. Motilal Vigyan Mahavidyalaya

College of India for their invaluable helpful discussions.

REFERENCES

1. P.P. Gunaicha, S. Gangam, J.L. Roehl, and S.V. Khare, *Sol. Energy* 102, 276 (2014).
2. O. Keng-Liang, J.-C. Fan, J.-K. Chen, C.-C. Huang, L.-Y. Chen, J.-H. Ho, and J.-Y. Chang, *J. Mater. Chem.* 22, 14667 (2012).
3. A. Nagaoka, K. Yoshino, H. Taniguchi, T. Taniyama, K. Kakimoto, and H. Miyake, *J. Cryst. Growth* 386, 204 (2014).
4. T.V. Vu, A.A. Lavrentyev, B.V. Gabrelian, K.D. Pham, C.V. Nguyen, K.C. Tran, H.L. Luong, M. Batouche, O.V. Parasyuk, and O.Y. Khyzhun, *J. Electr. Mater.* 48, 705 (2018).
5. K. Schwarz and P. Blaha, *Comput. Mater. Sci.* 28, 259 (2003).
6. K. Schwarz, *J. Solid State Chem.* 176, 319 (2003).
7. J.P. Perdew, A. Ruzsinszky, G.I. Csonka, O.A. Vydrov, G.E. Scuseria, L.A. Constantin, X. Zhou, and K. Burke, *PRL* 100, 136406 (2008).
8. J. Jonathan, *Scragg, Copper Zinc Tin Sulfide Thin Films for Photovoltaics* (Springer, Heidelberg Dordrecht London New York: Synthesis and Characterisation by Electrochemical Methods, 2011).
9. M.Y. Valakh, V.M. Dzhagan, I.S. Babichuk, X. Fontane, A. Perez-Rodriquez, and S. Schorr, *JETP Lett.* 98, 255 (2013).
10. J. He, L. Sun, N. Ding, H. Kong, S. Zuo, S. Chen, Y. Chen, P. Yang, and J. Chu, *J. Alloys Compd.* 529, 34 (2012).
11. L. Vegard, *Zeitschrift für Physik* 5, 17 (1921).
12. F.D. Murnaghan, *PNAS September 15* 30, 244 (1944).
13. S. Zamulko, K. Berland, and C. Pesson, *Phys. Status Solidi A* 215, 1700945 (2018).
14. A. Nagaoka, K. Yoshino, K. Aoyagi, T. Minemoto, Y. Nose, T. Taniyama, K. Kakimoto, and H. Miyake, *J. Cryst. Growth* 393, 167 (2014).
15. G. Kresse and J. Furthmüller, *Phys. Rev. B* 54, 11169 (1996).
16. S.V. Baryshev and E. Thimsen, *Chem. Mater.* 27, 2294 (2015).
17. T. Maeda, S. Nakamura, and T. Wada, *Mater. Res. Soc. Symp. Proc.* 1165, 1165-M04-03 (2009).
18. E. Chagarov, K. Sardashti, R. Haight, D.B. Mitzi, and A.C. Kummel, *J. Chem. Phys.* 145, 064704 (2016).
19. A. Walsh, S. Chen, S.-H. Wei, and X.-G. Gong, *Adv. Energy Mater.* 2, 400 (2012).
20. C. Dun, N.A.W. Holzwarth, Y. Li, W. Huang, and D.L. Carroll, *J. Appl. Phys.* 115, 193513 (2014).
21. A. Otero-de-la-Roza, D. Abbasi-Pérez, and V. Luaña, *Comput. Phys. Commun.* 182, 2232 (2011).
22. L. Samrath, *Chaplot, Ranjan Mittal, and Narayani Choudhury, Thermodynamic Properties of Solids, Experiment and Modeling* (Weinheim: WILEY-VCH Verlag GmbH & Co. KGaA, 2010).
23. M.A. Blanco, E. Francisco, and V. Luaña, *Comput. Phys. Commun.* 158, 57 (2004).
24. E. Efstathios, *(Stathis) Michaelides, Nanofluidics* (Springer Cham Heidelberg New York Dordrecht London: Thermodynamic and Transport Properties, 2014).
25. S. Adachi, *Earth-Abundant Materials for Solar Cells Cu2–II–IV–VI4 Semiconductors* (London: Wiley, 2015).